THE JOURNAL OF BIOLOGICAL CHEMISTRY
Vol. 274, No. 4, Issue of January 22, pp. 2145–2156, 1999

Printed in U.S.A.

Role of ERAB/L-3-Hydroxyacyl-coenzyme A Dehydrogenase Type II Activity in Aβ-induced Cytotoxicity*

(Received for publication, June 17, 1998, and in revised form, September 23, 1998)

Shi Du Yan‡, Yigong Shi§, Aiping Zhu, Jin Fu, Huaijie Zhu, Yucui Zhu, Lenneen Gibson, Eric Stern, Kate Collison¶, Futwan Al-Mohanna¶, Satoshi Ogawa‖, Alex Roher, Steven G. Clarke‡‡, and David M. Stern**

*From the Departments of Pathology, Physiology and Surgery, College of Physicians and Surgeons of Columbia University, New York, New York 10032, the ¶King Faisal Specialist Hospital and Research Centre, Riyadh, Saudi Arabia, the ‖Department of Anatomy and Neuroscience, Osaka University School of Medicine, Osaka, Japan, the §Department of Molecular Biology, Princeton University, Princeton, New Jersey 08544, the **Haldeman Laboratory for Alzheimer's Disease Research, Sun Health Research Institute, Sun City, Arizona 85372, and the ‡‡Department of Chemistry and Biochemistry, UCLA, Los Angeles, Calilfornia 90024*

Endoplasmic reticulum-associated amyloid β-peptide (Aβ)-binding protein (ERAB)/L-3-hydroxyacyl-CoA dehydrogenase type II (HADH II) is expressed at high levels in Alzheimer's disease (AD)-affected brain, binds Aβ, and contributes to Aβ-induced cytotoxicity. Purified recombinant ERAB/HADH II catalyzed the NADH-dependent reduction of *S*-acetoacetyl-CoA with a K_m of ≈68 μM and a V_{max} of ≈430 μmol/min/mg. The contribution of ERAB/HADH II enzymatic activity to Aβ-mediated cellular dysfunction was studied by site-directed mutagenesis in the catalytic domain (Y168G/K172G). Although COS cells cotransfected to overexpress wild-type ERAB/HADH II and variant β-amyloid precursor protein (βAPP(V717G)) showed DNA fragmentation, cotransfection with Y168G/K172G-altered ERAB and βAPP(V717G) was without effect. We thus asked whether the enzyme might recognize alcohol substrates of which the aldehyde products could be cytotoxic; ERAB/HADH II catalyzed oxidation of a variety of simple alcohols (C2–C10) to their respective aldehydes in the presence of NAD^+ and NAD-dependent oxidation of 17β-estradiol. Addition of micromolar levels of synthetic Aβ(1–40) to purified ERAB/HADH II inhibited, in parallel, reduction of *S*-acetoacetyl-CoA (K_i ≈ 1.6 μM), as well as oxidation of 17β-estradiol (K_i ≈3.2 μM) and (−)-2-octanol (K_i ≈ 2.6 μM). Because micromolar levels of Aβ were required to inhibit ERAB/HADH II activity, whereas Aβ binding to ERAB/HADH II occurred at much lower concentrations (K_m ≈ 40–70 nM), the latter more closely simulating Aβ levels within cells, Aβ perturbation of ERAB/HADH II was likely to result from mechanisms other than the direct modulation of enzymatic activity. Cells cotransfected to overexpress ERAB/HADH II and βAPP(V717G) generated malondialdehyde-protein and 4-hydroxynonenal-protein epitopes, which were detectable only at the lowest levels in cells overexpressing either ERAB/HADH II or βAPP(V717G) alone. Generation of such toxic aldehydes was not observed in cells contransfected to overexpress Y168G/K172G-altered ERAB and βAPP(V717G). We conclude that the generalized alcohol dehydrogenase activity of ERAB/HADH II is central to the cytotoxicity observed in an Aβ-rich environment.

Recent studies of mutations underlying familial Alzheimer's disease have strengthened links between amyloid β-peptide (Aβ)[1] and the pathogenesis of this devastating neurodegenerative disorder (1–6). Most work analyzing toxic effects of Aβ on cellular properties has employed high concentrations of Aβ fibrils that are thought to nonspecifically injure cells by destabilizing cell membranes (1, 4, 6–9). We have hypothesized, however, that early in Alzheimer's disease (AD), when levels of Aβ are much lower, the amyloidogenic peptide might interact with particular cellular target molecules, thereby magnifying the capacity of Aβ to perturb cellular functions (10–14). At the cell surface, receptors, for example, receptor for advanced glycation end products (RAGE), the p75 component of the neurotrophin receptor, and the macrophage scavenger receptor, are such molecular targets of Aβ (10–14). Another potential cellular interaction site is the endoplasmic reticulum-associated Aβ-binding protein, initially designated ERAB and first identified using the yeast two-hybrid system to screen for species that bound Aβ (15). ERAB was localized to the endoplasmic reticulum and mitochondria in cultured cells (15). Its expression was found to be increased in AD brain, and, *in vitro*, ERAB facilitated Aβ cytotoxicity in neuroblastoma and transfected COS cells. Our initial analysis of the ERAB amino acid sequence showed resemblance to the family of short-chain alcohol dehydrogenases, including hydroxysteroid dehydrogenases, Ke6, and acetoacetyl coenzyme A (CoA) reductases (16). These results suggested a primary role for ERAB in cell metabolism, in addition to having the potential to contribute to Aβ-induced cytotoxicity.

The bovine counterpart of ERAB was recently isolated from liver mitochondrial preparations, and characterized as the mitochondrial 3-hydroxyacyl-CoA dehydrogenase type II (HADH II) (E.C. 1.1.1.35) (17, 18), a participant in the third reaction of the fatty acid β-oxidation spiral (19, 20). This identification is

* This work was supported by Grants AG00690, AG14103, and AG11925 from the United States Public Health Service and by a grant from the Surgical Research Fund. The costs of publication of this article were defrayed in part by the payment of page charges. This article must therefore be hereby marked "*advertisement*" in accordance with 18 U.S.C. Section 1734 solely to indicate this fact.

‡ To whom correspondence should be addressed: Dept. of Pathology, P&S 17-410, College of Physicians & Surgeons of Columbia University, 630 West 168th St., New York, NY 10020. Tel.: 212-305-3958; Fax: 212-305-5337.

[1] The abbreviations used are: Aβ, amyloid β-peptide; AD, Alzheimer's disease; ERAB, endoplasmic reticulum-associated Aβ-binding protein; HADH II, L-3-hydroxyacyl-CoA dehydrogenase type II; HNE, 4-hydroxynonenal; MDA, malondialdehyde; mut, mutant; PDI, protein disulfide isomerase; wt, wild-type; RAI, relative apoptosis index; PAGE, polyacrylamide gel electrophoresis; ELISA, enzyme-linked immunosorbent assay; TUNEL, terminal deoxynucleotidyl transferase-mediated dUTP nick end labeling; MES, 4-morpholineethanesulfonic acid.

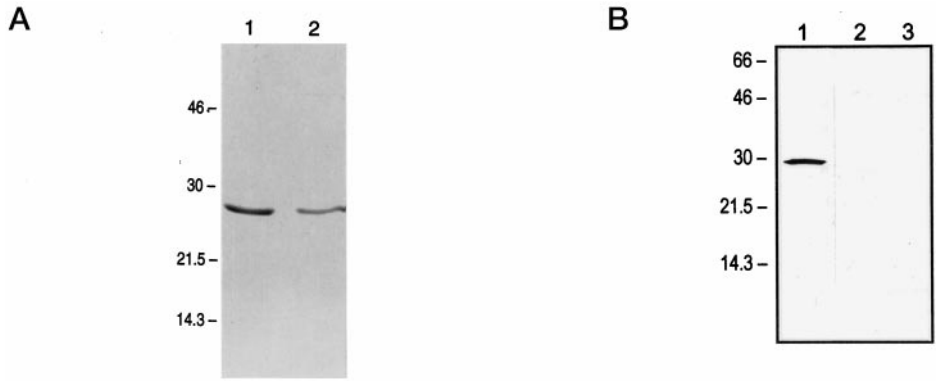

FIG. 1. **Characterization of *E. coli*-derived ERAB/HADH II.** *A,* nonreduced (*lane 1*) and reduced (*lane 2*) SDS-PAGE (12%) of purified recombinant ERAB/HADH II (1 μg/lane). Protein was visualized by Coomassie Blue staining. Standard proteins were run simultaneously, and their migration is indicated by the *bars* on the *far left*. Each *bar* is labeled with the corresponding molecular mass in kDa. B. Immunoblotting. Purified recombinant ERAB/HADH II was subjected to reduced SDS-PAGE (12%) followed by immunoblotting. ERAB antigen was visualized using rabbit anti-full-length recombinant ERAB/HADH II IgG (3.5 μg/ml) (*lane 1*), followed by application of secondary antibody and the detection system. In *lane 2*, excess soluble ERAB/HADH II (50-fold molar excess over the amount of primary antibody) was added during incubation of blots with the primary antibody. In *lane 3*, ERAB/HADH II was present on the membrane (as in *lane 1*), but the same amount preimmune IgG was used in place of immune IgG. Details of procedure are described in the text.

consistent with a recent report concerning properties of a human L-3-hydroxyacyl-CoA dehydrogenase (21), the cDNA sequence of which is identical to that of human ERAB.[2] Although consequences of ERAB/HADH II deficiency are not known, heritable disorders with defects in fatty acid β-oxidation have been identified (19, 20). These patients have hepatomegaly, cardiomegaly, encephalopathies, peripheral neuropathy, rhabdomyolysis, and myoglobinuria, suggesting a role for fatty acid β-oxidation enzymes in the metabolic balance of a range of organs.

To investigate whether the enzymatic activity of ERAB/HADH II was correlated with its interaction with Aβ and cytotoxicity, we have further characterized this protein. We find that it has the ability to catalyze the oxidation of alcohol groups in a range of substrates, including linear alcohols and estradiol, as well as the reduction of *S*-acetoacetyl-CoA. To analyze the role of ERAB/HADH II enzymatic activity in potentiation of Aβ toxicity, a catalytically crippled form was prepared containing two substitutions in the highly conserved sequence of residues 168–172 (YSASK), putatively assigned as part of the active center of the enzyme (16). Cells overexpressing mutant ERAB were relatively protected from Aβ cytotoxicity consequent to overexpression of mutant βAPP(V717G), as demonstrated by suppression of apoptosis. In contrast, cells overexpressing both wild-type ERAB/HADH II and βAPP (V717G) suffered increased cytotoxicity. Thus, it appears that activity of the enzyme is necessary for full toxicity. In cells overexpressing ERAB/HADH II and βAPP(V717G), the intracellular distribution of ERAB/HADH II was altered, and generation of reactive aldehydes, including malondialdehyde and 4-hydroxynonenal, occurred. Such reactive aldehydes provide a barometer of oxidant cell stress (22–25) and have been observed in the brain of AD patients (26–32). These data lead us to propose that enzymatically active ERAB/HADH II, an alcohol dehydrogenase with broad substrate specificity, may have a role in metabolic homeostasis but can switch to a pathologic role in an Aβ-rich environment, as in AD, potentiating cell stress and cytotoxicity.

[2] ERAB was the name applied to HADH II before their identity was ascertained. The designation ERAB/HADH II is used to emphasize the properties of ERAB with respect to binding of Aβ and potentiation of Aβ toxicity, as well as its metabolic function as a 3-hydroxyacyl-CoA dehydrogenase. We propose to rename the enzyme Aβ binding alcohol dehydrogenase as this reflects both its capacity to bind Aβ and its activity as a generalized alcohol dehydrogenase (see text).

EXPERIMENTAL PROCEDURES

Preparation of Wild-type and Mutant Forms of ERAB—Escherichia coli (BL21) was transformed with pGE5-human ERAB/HADH II or mutant forms of ERAB/HADH II, prepared as described below. Transformants were induced with 0.5 mM isopropyl-1-thio-β-D-galactopyranoside for 3 h, and cell extracts were prepared by cell disruption. Extracts were subjected to cation exchange FPLC chromatography on SP Sepharose Fast Flow (Amersham Pharmacia Biotech) and on Source 15S, followed by gel filtration on Superdex 200. The extract from ~1 liter of bacterial culture was applied to 2 ml of SP Sepharose in 25 mM MES (pH 6.0), 50 mM NaCl, 5 mM dithiothreitol. The resin was washed with equilibration buffer and eluted with an ascending linear salt gradient (0.1–1.0 M NaCl). ERAB/HADH II, detected by its migration on SDS-PAGE and by immunoblotting (see below), eluted in fractions corresponding to 0.15–0.4 M NaCl. These fractions were pooled, diluted 6-fold, and applied to Source 15S resin in 0.1 M MES (pH 6.0)/0.1 M NaCl (5 mg of protein per 1 ml of resin). The column was eluted with an ascending salt gradient, and ERAB/HADH II emerged at ≈0.15 M NaCl. ERAB/HADH II-rich fractions were concentrated by ultrafiltration to ≈15 mg/ml and loaded onto a Superdex 200 (30/10) column (1 ml was applied to the column for each run). Peak fractions from Superdex 200 were subjected to SDS-PAGE (12%) and immunoblotting. Immunodetection of ERAB/HADH II employed as primary antibody either anti-ERAB peptide IgG (15) or antibody prepared in rabbits, according to standard methods (33), using full-length recombinant human ERAB/HADH II as the immunogen. IgG was purified from rabbit antisera by chromatography on Protein A-Sepharose CL-4B (Amersham Pharmacia Biotech). Sites of primary antibody binding were visualized with peroxidase-conjugated goat anti-rabbit IgG (Sigma). The ERAB/HADH II immunoreactive band migrated with ≈27 kDa, consistent with previous observations (15, 17, 18, 21). N-terminal sequencing of wild-type and mutant forms of ERAB/HADH II was performed on a Porton 2090 E gas phase protein sequencer (Beckman) equipped with an on-line Hewlett-Packard 1090 HPLC. Site-directed mutagenesis was employed to mutate tyrosine (168) and/or lysine (172) to glycine using a kit from Promega (Madison, WI).

Assays of ERAB Enzymatic Activity and Aβ Binding—ERAB/HADH II was studied for its activity to reduce *S*-acetoacetyl-CoA, as well as its capacity to dehydrogenate alcohol groups in a range of linear alcohols and in estradiol. The assay for reduction of *S*-acetoacetyl-CoA employed ERAB/HADH II (333 ng/ml), a range of *S*-acetoacetyl-CoA concentrations (0.0015–0.36 mM; Sigma), and NADH (0.1 mM; Sigma) in 97 mM potassium phosphate (pH 7.3). The reaction was run for a total of 2 h at 25 °C under steady-state conditions (34), and the change in NADH absorbance at 340 nm was determined every 5 min. Alcohol dehydrogenase assays employed ERAB/HADH II (20 μg/ml), a range of alcohol substrates and concentrations (methanol, ethanol, *n*-propanol, isopropanol, *n*-butanol, isobutanol, *n*-pentanol, (±)-2-octanol, (+)-2-octanol, (−)-2-octanol, and *n*-decanol; Sigma), and NAD^+ (7.5 mM) in 22 mM sodium pyrophosphate, 0.3 mM sodium phosphate (pH 8.8). The reaction was run for 2 h at 25 °C, and the absorbance at 340 nm was monitored every 5 min as described above. Studies to evaluate oxidation

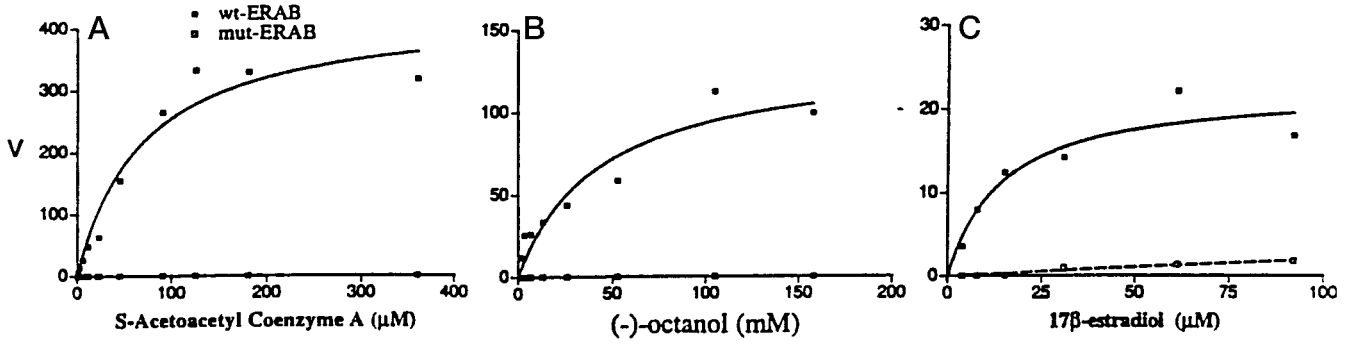

FIG. 2. **Characterization of ERAB/HADH II enzymatic activity: reduction of *S*-acetoacetyl-CoA (*A*) and oxidation of octanol (*B*) and 17β-estradiol (*C*).** Experiments utilized either wild-type ERAB/HADH II (*filled squares*) or mutant ERAB(Y168G/K172G) (*open squares*). The same concentration of wild-type and mutant ERAB was used in each case. *A,* ERAB/HADH II (0.33 μg/ml) was incubated with the indicated concentration of *S*-acetoacetyl-CoA and NADH (0.1 mM). *B,* ERAB/HADH II (20 μg/ml) was incubated with the indicated concentration of (−)-octanol and NAD^+ (7.5 mM). *C,* ERAB/HADH II (30 μg/ml) was incubated with the indicated concentration of 17β-estradiol and NAD^+ (0.4 mM). The velocity (*V*) of the reaction (units/mg of protein) is plotted *versus* added substrate concentration. Details of the experimental methods are described in the text. The *broken line* represents the theoretical curve according to the K_m and V_{max} values (see Table I) calculated by the computer program. Experimental procedures are described in the text.

of 17β-estradiol employed ERAB/HADH II (30 μg/ml), a range of 17β-estradiol concentrations (3.8–92 μM), and NAD^+ (0.4 mM) in 20 mM sodium pyrophosphate (pH 8.9) at 25 °C for 2 h. Where indicated, freshly prepared synthetic Aβ(1–40) or Aβ(1–42), either obtained from California Peptide Inc. (Napa, CA) and purified by reversed-phase and size exclusion high pressure liquid chromatography (purity was confirmed by mass spectrometry, amino acid analysis and peptide mapping) or purchased in purified form from QCB (Hopkinton, MA) was added to the reaction mixture. Aβ(1–40) was freshly prepared and dissolved in distilled water. Aβ(1–42) was also freshly prepared and dissolved in Me_2SO. The final concentration of Me_2SO was <1%, and control experiments using this concentration of Me_2SO alone (*i.e.* without Aβ(1–42)) had no effect on the reactions under study. Kinetic data were analyzed by PRISM (Scitech, San Diego, CA) to determine K_m, V_{max}, and K_i, and lines shown in the figures represent theoretical curves according to kinetic parameters calculated by the program. One unit of enzyme activity was defined as that converting 1.0 μmol of substrate to product per min. For K_i, a one-site competitive inhibition model was used (34).

Binding of ERAB/HADH II to Aβ was studied using ^{125}I-labeled purified recombinant ERAB/HADH II (15). The protein was labeled by the Iodobead method to a final specific radioactivity of ≈2000 cpm/ng (an average of five labelings) and the tracer was >90% precipitable in trichloroacetic acid (10%). Wells were incubated overnight at 4 °C with Aβ(1–40) diluted into carbonate buffer (0.1 M; pH 9.6). Excess sites in the well were blocked with phosphate-buffered saline containing fatty acid-free bovine serum albumin (10 mg/ml) for 2 h at 37 °C. Wells were aspirated, and binding buffer (minimal essential medium containing fatty acid-free bovine serum albumin, 1 mg/ml; 0.05 ml) was added with ^{125}I-ERAB/HADH II alone or in the presence of 100-fold excess unlabeled ERAB/HADH II. Binding was allowed to proceed for 2 h at 37 °C, and each well was washed four times (0.2 ml/wash) over 30 s with ice cold phosphate-buffered saline containing Tween 20 (0.05%). Bound tracer was eluted with Nonidet P-40 (1%) over 5 min at 37 °C. Specific binding was defined as total minus nonspecific binding. Total binding was that observed in the presence of tracer alone. Nonspecific binding was that observed with tracer in the presence of 100-fold excess unlabeled ERAB/HADH II. Binding experiments were performed with four replicates per concentration of tracer. Data were analyzed by nonlinear least squares analysis (Enzfitter) using a one-site model by the method of Klotz and Hunston (35).

Cell Transfection Studies—Transient transfection of COS-1 or neuroblastoma (N115) cells (ATCC) employed pcDNA3/human ERAB/HADH II (wild-type or mutant forms) using LipofectAMINE according to previously described methods (15). Where indicated, cultures were subjected to transient transfection with pAdlox/βAPP(V717G). The latter was made by inserting a construct encoding βAPP(V717G) (36) into the *Hin*dIII cloning sites in the pAdlox vector (37). Alternatively, a construct encoding wild-type (wt) βAPP(1–695) was inserted into the *Sal*I cloning sites of the pMT vector (38) to make pMT/wtβAPP. βAPP was detected with rabbit anti-C-terminal βAPP IgG (369W) generously provided by Dr. Sam Gandy (New York University, New York, NY) (39).

Assays for DNA Fragmentation and Subcellular Localization—The effect of ERAB/HADH II on cellular properties was determined in the absence and the presence of an Aβ-rich environment (the latter provided by transfection with pAdlox/βAPP(V717G)). COS and neuroblastoma cells transiently transfected with pcDNA3/ERAB with or without pAdlox/βAPP(V717G) were assayed for evidence of DNA fragmentation using the ELISA for cytoplasmic histone-associated DNA fragments (Cell Death ELISA; Boehringer Mannheim) and the TUNEL assay (Boehringer Mannheim). Similar experiments were performed employing pMT/wtβAPP in place of βAPP(V717G). In order to determine the relative apoptosis index (RAI) (15), cells were also evaluated for expression of ERAB/HADH II or βAPP immunocytochemically (cells were fixed in 2% paraformaldehyde containing 0.1% Nonidet P-40) using primary antibodies to each antigen and peroxidase-conjugated anti-rabbit IgG (Sigma) as the secondary antibody, (because both primary antibodies were prepared in rabbits, ERAB/HADH II and βAPP were detected separately in duplicate cultures; the TUNEL assay was performed on the same cultures in which ERAB/HADH II or βAPP was visualized.

Subcellular localization of ERAB/HADH II employed ultracentrifugation of disrupted cells and confocal microscopy. Cells (5×10^8) were transfected as above, and, 12 h later, cells were pelletted and fractionated as described (40). In brief, cell pellets frozen at −80 °C were thawed, resuspended in 10 ml of Buffer A (0.25 M sucrose; 10 mM HEPES, pH 7.5; 1 mM dithiothreitol; 1 mM phenylmethylsulfonyl fluoride, 1 μg/ml leupeptin; 0.1 mM 1-chloro-3-tosylamido-7-amino-2-heptanone), and cavitated at 400 p.s.i. for 30 min using a nitrogen cavitation bomb apparatus (Kontes Glass Co., Vineland, NJ). Following cell disruption, the lysate was clarified by centrifugation at 10,000 × *g* for 15 min at 4 °C, and the pellet was resuspended in TNE buffer (10 mM Tris-HCl, pH 8.0; 1% Nonidet P-40; 150 mM NaCl; 1 mM EDTA; 10 μg/ml aprotinin; 1 mM phenylmethylsulfonyl fluoride). The latter material was centrifuged and fractionated through a series of sucrose steps (38, 30, and 20% sucrose prepared in 10 mM HEPES, pH 7.5; 1 mM dithiothreitol) at 100,000 × *g* for 3 h at 4 °C. Layered fractions (fractions 1–4) were collected by puncturing the tube at the desired depth and gently withdrawing the fluid. The pellet at the bottom of the tube was resuspended in 3 ml of Buffer A (precipitate fraction, termed fraction 5). Following determination of protein content, each fraction (5 μg protein/lane) was subjected to Western blotting using anti-ERAB/HADH II IgG. Enrichment of cellular structures/organelles in subcellular fractions was identified by the presence of marker proteins: RAGE (control cultures were transfected with pcDNA3/RAGE that was detected by Western blotting using specific antibodies to RAGE (10) in order to identify the plasma membrane-rich fraction), GRP78/Bip (endoplasmic reticulum; StressGen; Victoria, Canada) (40), and cytochrome *c* (mitochondria; StressGen). The mitochondria-rich fraction was also prepared using the method of Du *et al.* (41).

Confocal microscopy (Zeiss) employed rabbit anti-human ERAB/HADH II IgG, monoclonal antibody to protein disulfide isomerase (PDI) (StressGen) and a specific marker for mitochondria (Mito-Tracker™ Red CMXRos, Molecular Probes, Eugene, OR). For detection of malondialdehyde (MDA) and 4-hydroxynonenal (HNE) epitopes, murine monoclonal anti-MDA-lysine IgG (1 μg/ml; MDA2) and murine monoclonal anti-HNE-lysine IgG (1 μg/ml; NA59) were used, respectively (22–25). Antibodies were generated in the Immunology Core of the La

TABLE I
ERAB/HADH II activity

Substrate or alcohol	K_m	V_{max}	k_{cat}[a]	Catalytic efficiency, k_{cat}/K_m
	mM	*units/mg*	s^{-1}	$M^{-1}s^{-1}$
Reduction of *S*-acetoacetyl-CoA[b]				
S-Acetoacetyl-CoA	0.068 ± 0.020	430 ± 45	190	2.8×10^6
Oxidation of alcohol substrates[b]				
17β-Estradiol	0.014 ± 0.006	23 ± 3	10	7.4×10^5
Methanol	No activity	No activity	No activity	No activity
Ethanol	1210 ± 260	2.2 ± 0.4	1.0	0.82
Isopropanol	150 ± 17	36 ± 2	16	110
n-Propanol	272 ± 62	4.2 ± 0.5	1.9	6.9
n-Butanol	53 ± 6	9.0 ± 0.3	4.0	76
Isobutanol	56 ± 16	8.0 ± 0.7	3.6	64
n-Pentanol	18 ± 5	6.9 ± 0.4	3.1	170
(±)-2-Octanol	85 ± 17	245 ± 20	110	1300
(+)-2-Octanol	84 ± 16	102 ± 8	46	540
(−)-2-Octanol	43 ± 9.0	133 ± 23	60	1400
n-Decanol	14 ± 6.3	2.8 ± 0.5	1.3	90

[a] Calculation based on 1 unit representing one μmol of product formed per min and a molecular mass of the enzyme as 26,926 Da.
[b] Experiments were performed by incubating ERAB/HADH II with a range of concentrations of the indicated substrates in the presence of NAD/NADH. Details of experimental procedures are described in the text.

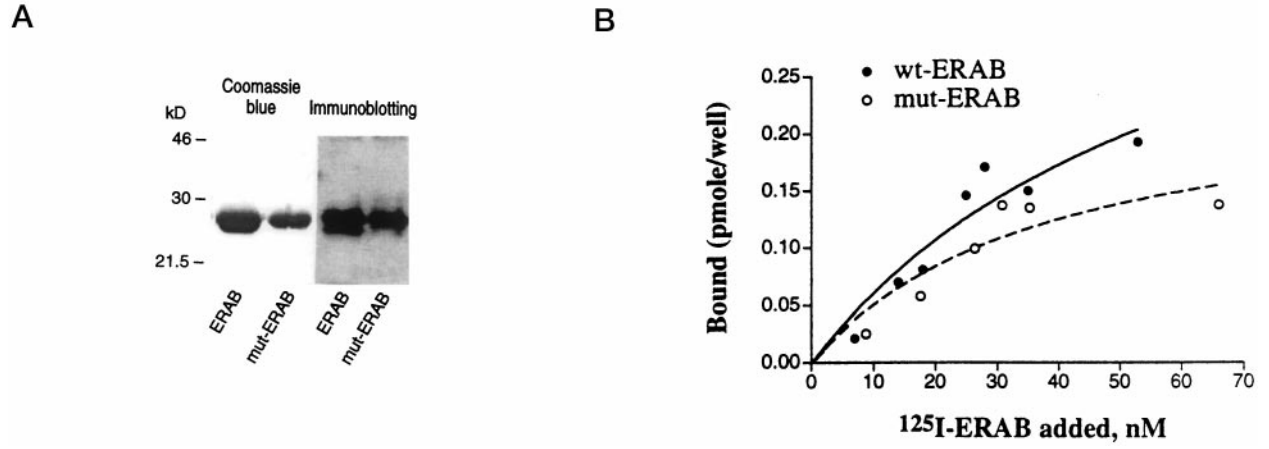

FIG. 3. **Characterization of mutant ERAB/HADH II (Y168G/K172G).** *A, left two lanes,* reduced SDS-PAGE (12%) of wild-type ERAB (ERAB/HADH II) and mutERAB/HADH II (5 μg/lane). Protein was visualized by Coomassie Blue staining. *A, right two lanes,* SDS-PAGE of ERAB/mutERAB (as above) followed by immunoblotting with anti-ERAB/HADH II IgG. Migration of simultaneously run molecular mass markers is indicated on the left in kilodaltons (*kD*). *B,* binding of ^{125}I-ERAB/HADH II to Aβ(1–40). Wells were incubated with Aβ (5 μg/ml), followed by blocking excess sites in the well with albumin-containing buffer and then addition of ^{125}I-ERAB/HADH II (either wild-type or mutERAB) alone or in the presence of 100-fold molar excess of unlabeled ERAB/HADH II (either wild-type or mutERAB). Specific binding (total minus nonspecific binding) is plotted *versus* added ERAB/HADH II (nM). The *broken line* shows the best-fit line by nonlinear least squares analysis.

Jolla SCOR in Molecular Medicine and Atherosclerosis and were kindly supplied by Dr. Joe Witztum (University of California, San Diego, CA). Cultures were fixed using 4% paraformaldehyde plus 5% sucrose (pH 7.4) containing 50 μM butylated hydroxytoluene and 1 mM EDTA (22–23). Sites of primary antibody binding were visualized by addition of rhodamine-conjugated goat anti-mouse IgG (Sigma). Confocal microscopy images were quantitated using the National Institutes of Health Image program.

RESULTS

Characterization of Recombinant Wild-type and Mutant Forms of ERAB/HADH II—E. coli was transformed with a plasmid encoding wt human ERAB/HADH II, and lysates were prepared. The recombinant protein was purified by sequential SP Sepharose and Source 15S chromatography, followed by gel filtration on Superdex 200. The final material was homogeneous on SDS-PAGE, displaying a single band migrating at an apparent molecular mass of ≈27 kDa (Fig. 1*A*), and, on amino acid sequencing, only the N-terminal sequence of ERAB/HADH II was obtained: Ala-Ala-Ala-Cys-Arg-Ser-Val-Lys-Gly Leu-Val-Ala-Val-Ile-Thr-Gly-Gly-Ala-Ser-Gly-Leu. Immunoblotting with anti-human ERAB IgG (Fig. 1*B, lane 1*) confirmed the presence of ERAB/HADH II epitopes in the recombinant ERAB/HADH II preparations. Addition of excess free ERAB/HADH II during incubation of blots with the primary antibody prevented appearance of the ERAB/HADH II-immunoreactive band (Fig. 1*B, lane 2*). Preimmune antibody did not visualize the ERAB/HADH II band on blots (Fig. 1*B, lane 3*).

Initial comparison with Swiss-Prot and Protein Data Bank using the FASTA algorithm indicated that the ERAB sequence most closely resembled the family of short-chain alcohol dehydrogenases, including hydroxysteroid dehydrogenases and acetoacetyl-CoA reductases (15). Studies of bovine HADH II, the bovine counterpart of ERAB, demonstrated that it possesses 3-hydroxyacyl-CoA dehydrogenase activity, catalyzing both forward and reverse reactions (18). In this work, we show that in the presence of NADH, ERAB reduced *S*-acetoacetyl-CoA with a K_m of ≈68 μM and a V_{max} of ≈430 units/mg (Fig. 2*A* and Table I). These values are similar to bovine HADH type II (K_m of ≈20 μM and V_{max} of ≈530 units/mg) (18), and to those of human HADH type II (HADH II) described in a report published during preparation of our manuscript (21). Thus, ERAB is an HADH and, based on amino acid sequence, is identical to human HADH type II. However, the interaction of ERAB with Aβ results in quite unexpected properties compared with what might be expected for a metabolic enzyme, leading us to term it

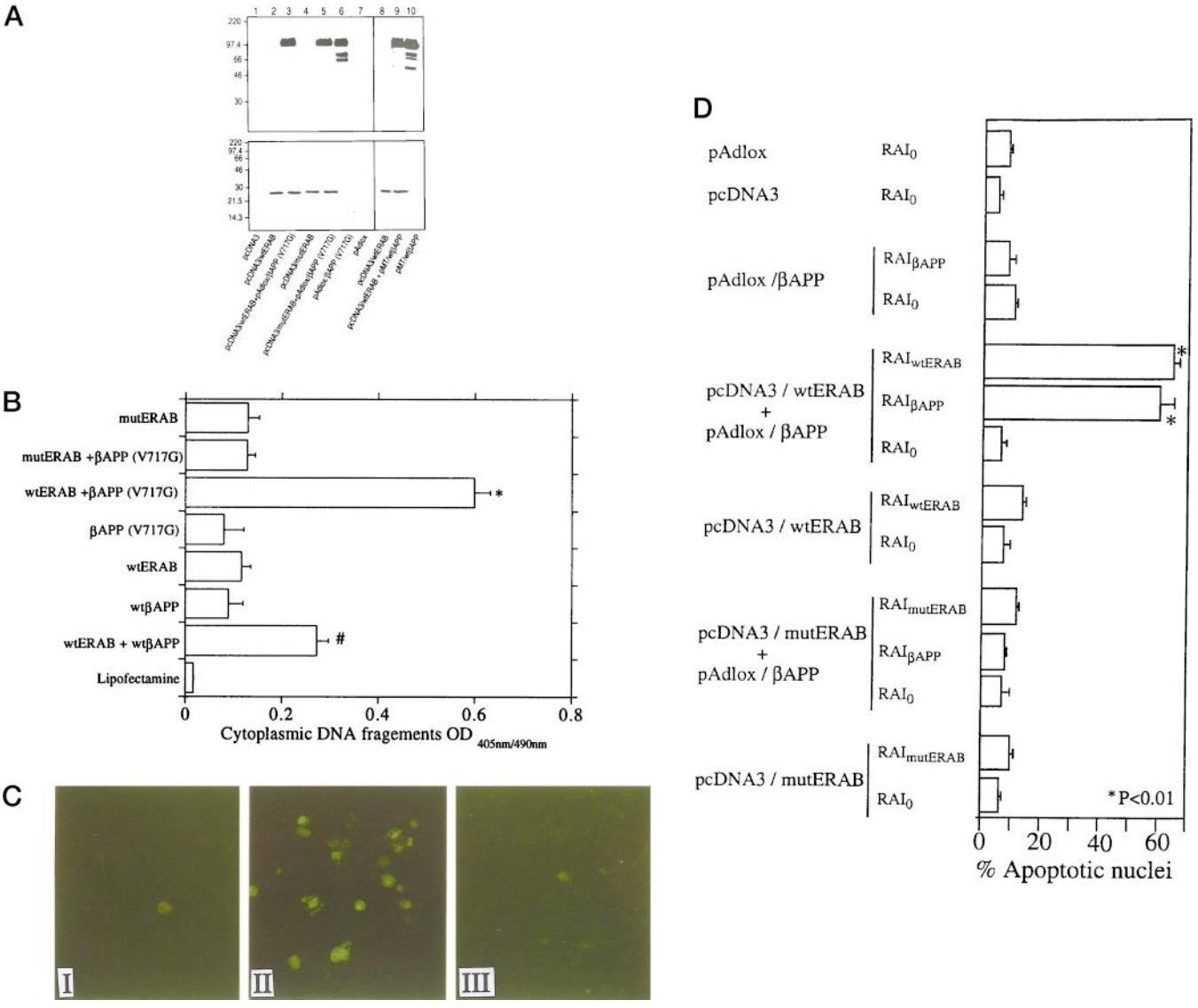

FIG. 4. **Cotransfection of COS cells to overexpress ERAB/HADH II and βAPP(V717G).** *A,* immunoblotting for βAPP (*top panel*) and ERAB/HADH II (*bottom panel*). Lysates of transiently transfected COS cells were subjected to SDS-PAGE (10% for βAPP, and 12% for ERAB/HADH II) followed by immunoblotting using antibody to βAPP (369W) (*top panel*) or antibody to ERAB/HADH II (*bottom panel*). Either the mutant form of βAPP(V717G) or wtβAPP was overexpressed. Lanes correspond to samples from COS cells transfected with the following constructs in the left panels: *lane 1,* pcDNA3; *lane 2,* pcDNA3/wtERAB; *lane 3,* pAdlox/βAPP(V717G) + pcDNA3/wtERAB; *lane 4,* pcDNA3/mutERAB; *lane 5,* pAdlox/βAPP(V717G) + pcDNA3/mutERAB; *lane 6,* pAdlox/βAPP(V717G); *lane 7,* pAdlox; *lane 8,* pcDNA3/wtERAB; *lane 9,* pMT/wtβAPP + pcDNA3/wtERAB; *lane 10,* pMT/wtβAPP. *B,* ELISA for cytoplasmic histone-associated DNA fragments. COS cells were transfected/cotransfected with plasmids resulting in overexpression of the indicated protein (wtERAB/HADH II, mutERAB, βAPP(V717G), or wtβAPP) or with LipofectAMINE alone. At the *far left,* the transfected gene product(s) are indicated. After 48 h, samples were harvested for the ELISA. * denotes $p < 0.01$; # denotes $p < 0.05$. *C,* TUNEL assay. COS cells were transfected with pcDNA3/wtERAB alone (*I*), pcDNA3/wtERAB + pAdlox/βAPP(V717G) (*II*), or pAdlox/βAPP(V717G) alone (*III*). Forty-eight hours later, the TUNEL assay was performed. *D,* RAI. Cells were transfected/cotransfected with the indicated constructs, and 48 h later, cultures were subjected to the TUNEL assay and immunostained to detect ERAB/HADH II or βAPP antigen (ERAB/HADH II and βAPP antigens were determined in duplicate cultures; ERAB/HADH II immunostaining and TUNEL assay, or βAPP immunostaining and TUNEL assay, were performed on the same slide). The RAI is a percentage denoting the ratio of the number of TUNEL positive nuclei in cells with the indicated antigen divided by the total number of cells with the indicated antigen in the same cell population. RAI_0 indicates the fraction of TUNEL positive nuclei in cells not staining for the transfected antigen divided by the total number of cells not expressing the indicated antigen in the same cell population. The constructs used for transfection/cotransfection are indicated on the far left.

ERAB/HADH II (to emphasize Aβ-induced modulation of its properties, see below). These data suggested the importance of determining the contribution of ERAB/HADH II enzymatic activity to its role in potentiation of Aβ cytotoxicity.

ERAB/HADH II Activity Is Essential for Promotion of Aβ Cytotoxicity—Tyr^{168} and Lys^{172} are part of a highly conserved sequence (residues 168–172) that has been putatively assigned as part of the active site of the enzyme (16). Thus, to prepare an active site-blocked form of human ERAB/HADH II, we mutated these residues simultaneously or separately by site-directed mutagenesis to Gly. Mutant (mut) ERAB(Y168G/K172G) was expressed in *E. coli* and purified as described above for wtERAB/HADH II. The final material was homogeneous on SDS-PAGE (Fig. 3*A, two left lanes*), migrated virtually identically with wtERAB/HADH II, had the expected N-terminal sequence (data not shown), and was immunoreactive with anti-ERAB IgG (Fig. 3*A, two right lanes*). Purified mutERAB(Y168G/K172G) was devoid of activity toward *S*-acetoacetyl-CoA (Fig. 2*A*), as well as octanol and 17β-estradiol (Fig. 2, *B–C*; see below). However, mutERAB bound Aβ in a manner comparable to wild-type ERAB (Fig. 3*B*); apparent K_d values for ERAB/HADH II binding to immobilized Aβ(1–40) were 64.5 ± 9.0 and 38.9 ± 9.3 nM for wild-type and mutant ERAB/HADH II, respec-

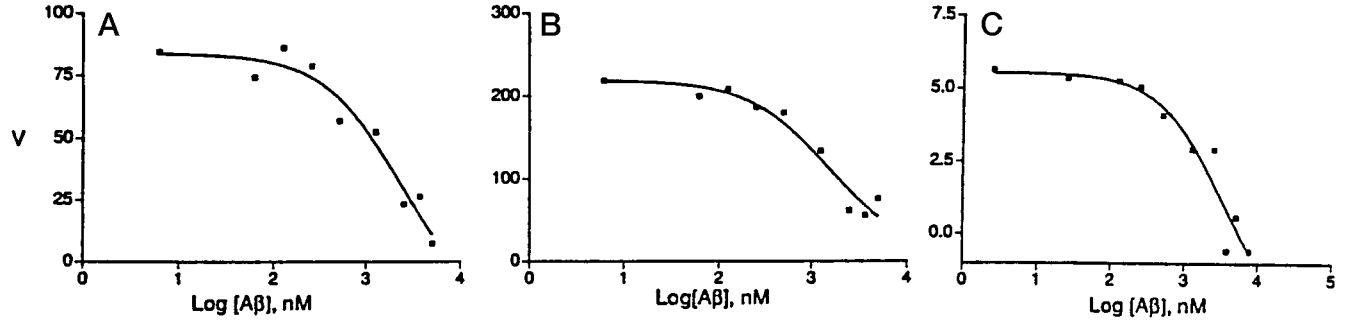

FIG. 5. **Effect of Aβ(1–40) on ERAB/HADH II enzymatic activity.** *A,* reduction of *S*-acetoacetyl-CoA. ERAB/HADH II (0.67 μg/ml) was incubated with *S*-acetoacetyl-CoA (0.18 mM), NADH (0.1 mM), and the indicated concentrations of Aβ. *B,* oxidation of octanol. ERAB/HADH II (10 μg/ml) was incubated with (−)-octanol (210 mM), NAD^+ (7.5 mM), and the indicated concentrations of Aβ. *C,* oxidation of 17β-estradiol. ERAB/HADH II (25 μg/ml) was incubated with 17β-estradiol (61 μM), NAD^+ (0.4 mM), and the indicated concentrations of Aβ. Velocity (*V*) of the reaction (units/mg of protein) is plotted *versus* log [Aβ] (nM). Data were fit to a one-site model for competitive inhibition.

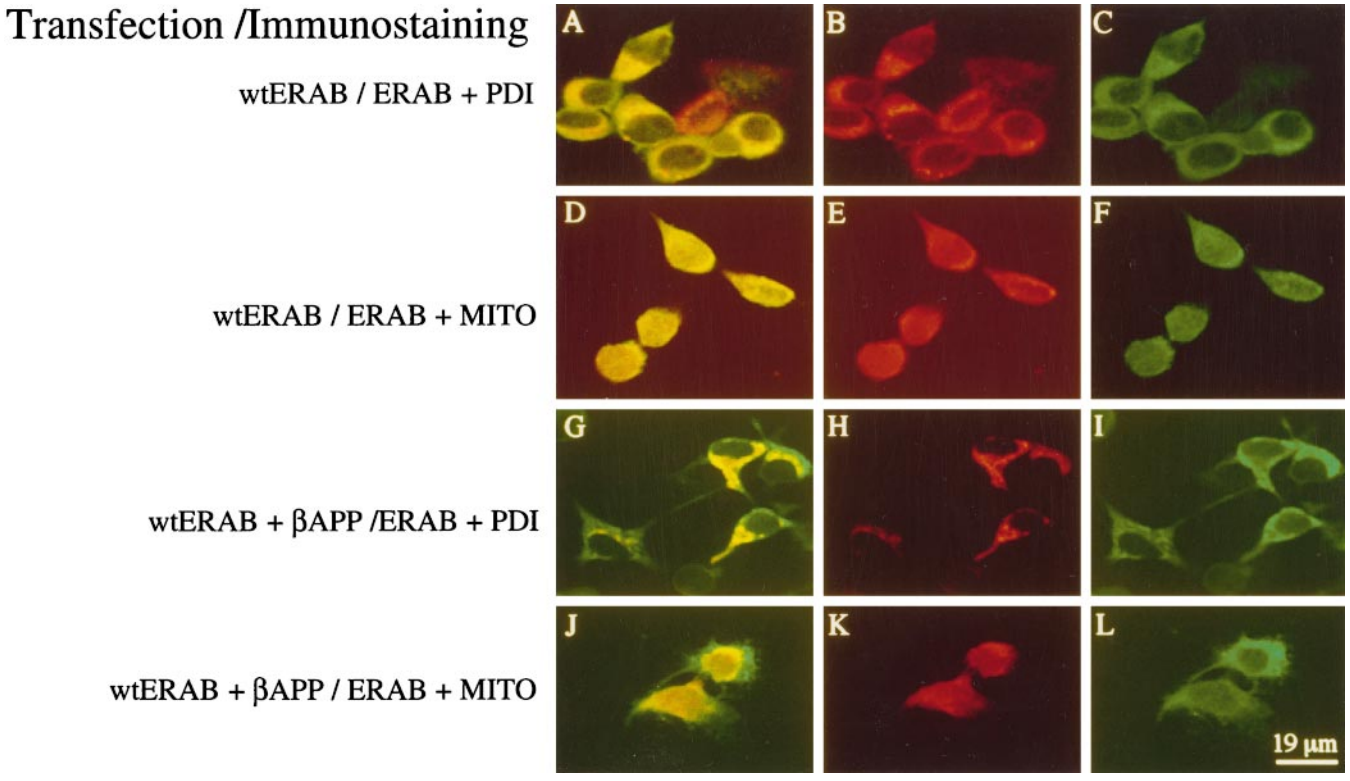

FIG. 6. **Subcellular distribution of ERAB/HADH II in neuroblastoma cells following transient transfection with or without βAPP(V717G).** *A–F,* neuroblastoma cells were transfected with pcDNA3/wtERAB/HADH II alone, and cultures were stained to visualize ERAB/HADH II + endoplasmic reticulum marker PDI (*A*), PDI alone (*B*), ERAB/HADH II alone (*C*), ERAB/HADH II + mitochondrial marker (*D*), mitochondrial marker alone (*E*), or ERAB/HADH II alone (*F*). *G–L,* neuroblastoma cells were cotransfected with pcDNA3/wtERAB + pAdlox/βAPP(V717G), and cultures were stained to visualize ERAB/HADH II + PDI (*G*), PDI alone (*H*), ERAB/HADH II alone (*I*), ERAB/HADH II + mitochondrial marker (*J*), mitochondrial marker alone (*K*), or ERAB/HADH II alone (*L*). On the *left* of the figure, the transfected gene products and the antigens visualized by immunostaining are indicated in the corresponding set of three panels.

tively. Similar binding of ERAB/HADH II to β-amyloid was observed with Aβ(1–42) (data not shown). Thus, mutERAB(Y168G/K172G) was an inactive form of the enzyme that retained the ability to interact with Aβ, allowing us to probe the role of ERAB/HADH II enzymatic activity in potentiation of Aβ cytotoxicity. Similar results were independently obtained with the two other ERAB/HADH II mutants, Y168G and K172G; in each case, the mutant form was devoid of enzymatic activity but retained the capacity to bind Aβ.

Recent studies have demonstrated that processing of βAPP, with generation of Aβ, can occur within multiple intracellular compartments (36, 42–46), including endoplasmic reticulum, a site where ERAB/HADH II has been localized. In particular, a construct encoding the London mutant of βAPP(V717G) forms increased levels of Aβ(1–42) in endoplasmic reticulum following transient transfection (36). This led us to develop a model system using COS and neuroblastoma cells for testing the effects of ERAB/HADH II on Aβ-induced cytotoxicity by cotransfection with plasmids causing overexpression of wild-type or mutant ERAB/HADH II and βAPP(V717G). First, expression of ERAB/HADH II and βAPP was evaluated under our experimental conditions by immunoblotting using antibody to ERAB/HADH II and C-terminal βAPP antibody (396W) (39). COS cells transiently transfected with pAdlox/βAPP(V717G) overexpressed βAPP antigen (Fig. 4*A, upper panel, lanes 3, 5,* and *6*), compared with controls (Fig. 4*A, upper panel, lanes 1, 2, 4,* and *7*), whether cells were cotransfected to overexpress wtERAB or mutERAB (Fig. 4*A, upper panel, lanes 3* and *5*) or not (Fig. 4*A, upper panel, lane 6*). Several closely spaced βAPP-immunoreactive bands with molecular masses of ≈110–140

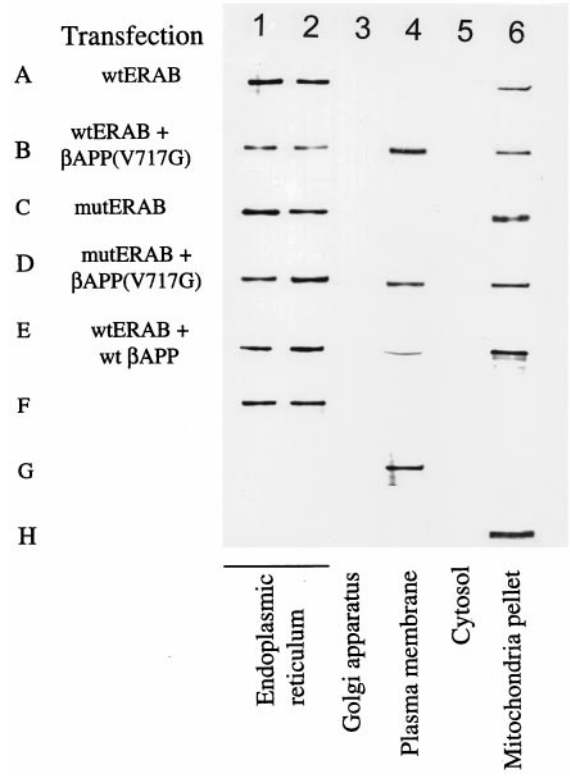

FIG. 7. Subcellular fractionation of neuroblastoma cells either transfected with pcDNA3/wtERAB/HADH II alone (*A*), cotransfected with pcDNA3/wtERAB + pAdlox/βAPP(V717G) (*B*), transfected with pcDNA3/mutERAB alone (*C*), cotransfected with pcDNA3/mutERAB + pAdlox/βAPP(V717G) (*D*), or cotransfected with pcDNA3/wtERAB/HADH II + pMT/wtβAPP (*E*). Neuroblastoma cells were transfected/cotransfected with the indicated constructs and processed as described in the text. Each fraction prepared from nontransfected neuroblastoma cells was also subjected to Western blotting using antibodies to ERAB/HADH II and/or to proteins associated with specific subcellular structures: GRP78/Bip for endoplasmic reticulum (*F, lanes 1* and *2*), RAGE for plasma membrane (*G, lane 4*), and cytochrome *c* for mitochondria (*H, lane 6*).

kDa (often coalescing into one broad band) (39) were seen, although more rapidly migrating immunoreactive forms of βAPP were also observed (Fig. 4*A, lane 6*). The latter forms were more evident in cells expressing βAPP(V717G) alone (Fig. 4*A, lane 6*) compared with those co-expressing βAPP(V717G) and wild-type or mutant ERAB/HADH II (although levels of the latter forms were comparable in cells overexpressing wtERAB/HADH II + βAPP(V717G) or mutERAB/HADH II + βAPP(V717G)) (Fig. 4*A, lanes 3* and *5*). Similarly, human ERAB/HADH II antigen was overexpressed by COS cells transfected with pcDNA3/wtERAB (Fig. 4*A, lower panel, lanes 2* and *3*) or pcDNA3/mutERAB (Fig. 4*A, lower panel, lanes 4* and *5*), whether cotransfected with pAdlox/βAPP(V717G) (Fig. 4*A, lower panel, lanes 3* and *5*) or not (Fig. 4*A, lower panel, lanes 2* and *4*). Comparable results were observed in cotransfection studies with neuroblastoma cells, although the absolute amount of the transfected gene products, βAPP and/or ERAB/HADH II, was somewhat less in neuroblastoma than in COS cells. Further experiments were performed with COS cells overexpressing wtβAPP following transfection with pMT/wtβAPP alone or cotransfection with pMT/wtβAPP + wtERAB/HADH II. Immunoblotting showed wtβAPP (Fig. 4*A, upper panel, lanes 9* and *10*) to be expressed at levels comparable to mutant βAPP (*lanes 3, 5,* and *6*), whether wtERAB/HADH II was present (*lane 9*) or not (*lane 10*). Similarly, cotransfection of COS cells with pMT/wtβAPP did not alter expression of wild-type ERAB/HADH II (Fig. 4*A, lower panel, lanes 8* and *9*).

COS cells cotransfected to overexpress wtERAB/HADH II and βAPP(V717G) displayed increased DNA fragmentation, as shown by ELISA for cytosolic histone-associated DNA fragments (Fig. 4*B*) and TUNEL assay (Fig. 4C, *I-III*, depicting representative fields of cells overexpressing wtERAB/HADH II alone (*I*), βAPP(V717G) alone (*III*), or wtERAB+βAPP(V717G) (*II*)). When COS cells were cotransfected to overexpress wtERAB with wtβAPP (the latter in place of mutant βAPP), evidence of increased DNA fragmentation was also observed compared with cultures overexpressing either wtERAB or wtβAPP alone (Fig. 4*B*). However, somewhat lower levels of DNA fragmentation were observed following overexpression of wtβAPP compared with βAPP(V717G), consistent with the previously observed higher levels of intracellular Aβ (especially Aβ(1–42) in endoplasmic reticulum) with this mutant form of βAPP (36).

In order to further validate these data, it was necessary to correlate cells expressing the transfected genes (by immunocytochemistry for ERAB/HADH II or βAPP) with those undergoing nuclear DNA fragmentation (by TUNEL assay). This was especially important, as the transient transfection system employed for these studies has an efficiency of ≈20–25%. For this reason, we utilized a RAI (15) to compare, in the same population, cells successfully transfected to overexpress wild-type/mutant ERAB/HADH II or βAPP and those undergoing apoptosis (Fig. 4*D*). The RAI denotes a ratio of cells with TUNEL-positive nuclei overexpressing ERAB/HADH II (RAI_{ERAB}) or βAPP ($RAI_{\beta APP}$) divided by the total number of cells expressing either ERAB/HADH II or βAPP. RAI_0 is the percentage of TUNEL-positive nuclei in cells in the same wells that did not express the transfected gene products, divided by the total number of cells that had negligible levels of these protein products. Cells transfected with pcDNA3/wtERAB alone displayed a low level of DNA fragmentation ($RAI_{ERAB} \approx 13\%$), similar to that observed in nontransfected cells in the same wells ($RAI_0 \approx 8\%$). Comparable results were observed when cells were transfected to overexpress βAPP(V717G) alone; $RAI_{\beta APP}$ was low, at ≈9%, and $RAI_{\beta APP} \approx RAI_0$ (11%). In contrast, COS cells cotransfected with pcDNA3/wtERAB + pAdlox/βAPP(V717G) had high levels of DNA fragmentation ($RAI_{ERAB} \approx 64\%$ and $RAI_{\beta APP} \approx 60\%$, the latter in separate experiments) compared with unsuccessfully transfected cells in the same well ($RAI_0 \approx 7\%$). These data indicate that overexpression of wtERAB along with mutant βAPP markedly enhanced cellular toxicity compared with either alone. Similar results were observed with neuroblastoma cells.

Using this experimental system, the effect of mutERAB (Y168G/K172G), in place of wtERAB/HADH II, was assessed in COS cells overexpressing βAPP(V717G). As noted above, levels of ERAB/HADH II in COS cells transfected with pcDNA3/mutERAB were comparable to those observed in COS cells transfected with pcDNA3/wtERAB (Fig. 4*A, lower panel*). Also, cotransfection of pcDNA3/mutERAB + pAdlox/βAPP(V717G) resulted in expression of βAPP antigen at levels comparable to those seen in cells transfected with the construct encoding wtERAB/HADH II (Fig. 4*A, upper panel*). However, cotransfection of COS cells with pcDNA3/mutERAB + pAdlox/βAPP(V717G) did not show an increase in cytoplasmic histone-associated DNA fragments, compared with cells transfected with pAdlox/βAPP(V717G) alone or other controls (Fig. 4*B*). Furthermore, using the RAI, cells cotransfected to overexpress βAPP(V717G) and mutERAB did not display an increase in RAI_{ERAB} (≈12%) or $RAI_{\beta APP}$ (≈9%), compared with RAI_0 (≈5%) (Fig. 4*D*). Thus, although mutERAB (Y168G/K172G) was expressed similarly to wtERAB/HADH II, the enzymati-

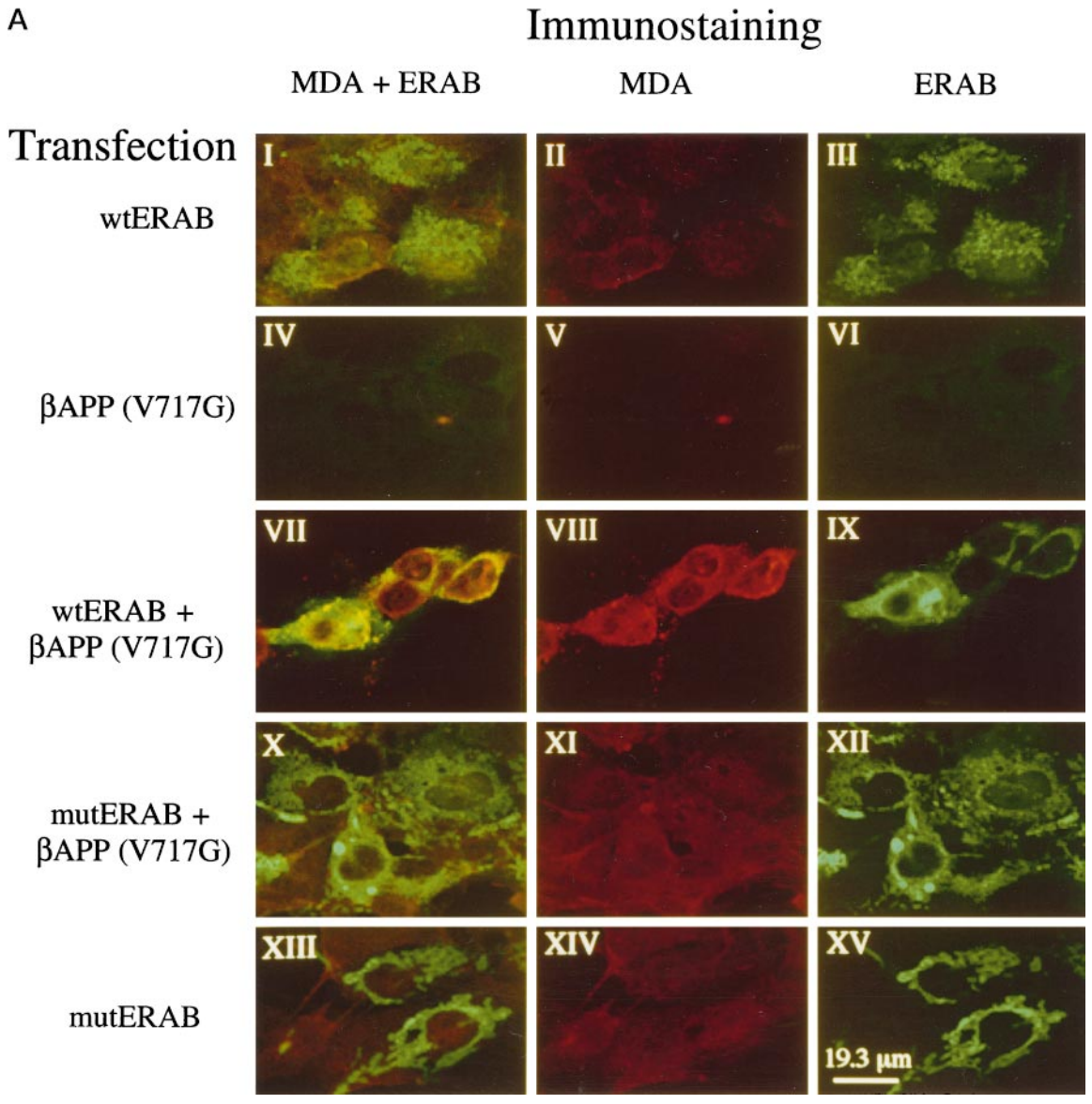

FIG. 8. **Expression of MDA and HNE epitopes in COS cells expressing wt or mutERAB/HADH II with or without βAPP(V717G).** COS cells were transiently transfected with pcDNA3/wtERAB or pcDNA3/mutERAB(Y168G/K172G) either alone or in the presence of pAdlox/βAPP(V717G). Cultures were fixed and stained with antibodies to MDA and ERAB/HADH II, or HNE and ERAB/HADH II. Panels represent the following. *A, I–IX,* MDA and ERAB/HADH II staining (wtERAB/HADH II): cells were transfected with pcDNA3/wtERAB alone (*I–III*), transfected with pAdlox/βAPP(V717G) alone (*IV–VI*), or cotransfected with pcDNA3/wtERAB + pAdlox/βAPP(V717G) (*VII–IX*). Cultures were stained to visualize either ERAB/HADH II alone (*green*) (*III, VI,* and *IX*), MDA alone (*red*) (*II, V,* and *VIII*) or ERAB/HADH II + MDA antigens (*I, IV,* and *VII*). *A, X–XV,* MDA and ERAB/HADH II (mutERAB) staining: cells were transfected with pcDNA3/mutERAB alone (*XIII–XV*) or cotransfected with pcDNA3/mutERAB + pAdlox/βAPP(V717G) (*X–XII*). Cultures were stained to visualize either ERAB/HADH II alone (*green*) (*XII* and *XV*), MDA alone (*red*) (*XI* and *IV*) or ERAB/HADH II + MDA antigens (*X* and *XIII*). *B, I–IX,* HNE and ERAB/HADH II (wtERAB) staining: staining was identical to *panel A,* except that antibody to HNE was used in place of antibody to MDA. B, *X–XV,* HNE and ERAB/HADH II staining (mutERAB): staining was identical to *panel A,* except that antibody to HNE was used in place of antibody to MDA. In each case, the antigens visualized by immunostaining (labeled *above* the figure) and the gene products overexpressed by transfection (labeled on the *far left*) are indicated.

cally inactive form was ineffective for potentiating apoptosis in COS cells overexpressing βAPP(V717G). Comparable results were observed when mutERAB(Y168G/K172G) was replaced with the two other mutant forms of ERAB/HADH II, Y168G and K172G (data not shown).

ERAB/HADH II Oxidation of Linear Alcohol Substrates and the Effect of Aβ—To probe mechanisms through which ERAB/HADH II induced its toxic effects in an Aβ-rich environment, possible dehydrogenation of a range alcohol substrates was studied, based on the hypothesis that such activity might give rise to aldehydes with associated toxic properties. Using a series of alcohols with carbon chains of differing lengths, ERAB/HADH II-dependent oxidation was evaluated; the most favorable catalytic efficiencies were seen for the stereoisomers of 2-octanol, with k_{cat}/K_m of ≈540–1400 M^{-1} s^{-1} and K_m values of ≈40–80 mM (Fig. 2*B* and Table I). ERAB/HADH II activity toward steroid substrates was studied using 17β-estradiol (Fig. 2*C*), NAD^+-dependent dehydrogenation occurred with a catalytic efficiency (k_{cat}/K_m) of ≈7.4×10^5 M^{-1} s^{-1} had a K_m value of ≈14 μM (see Table I). It is significant that this latter catalytic efficiency is only about 4-fold less than that seen in the reduction of *S*-acetoacetyl-CoA (Table I). These data were consistent with the concept that ERAB/HADH II could effectively metabolize a range of alcohols, although the activity toward linear alcohol substrates was less than that as an hydroxysteroid dehydrogenase.

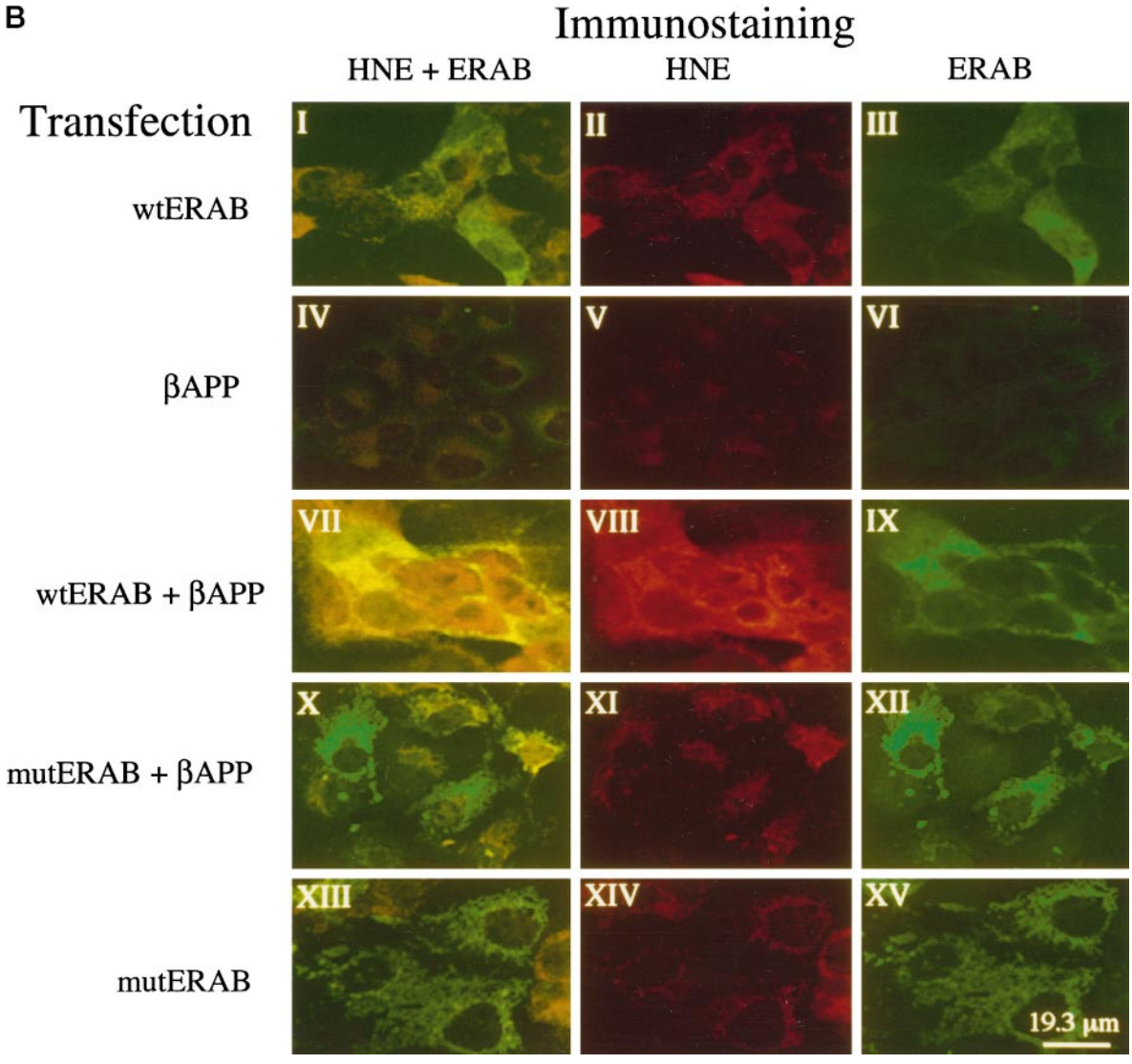

FIG.8—*continued*

Because enzymatic activity of ERAB/HADH II was essential for potentiation of Aβ cytotoxicity, it was possible that the amyloidogenic peptide enhanced the enzymatic activity of ERAB/HADH II or modulated substrate specificity, possibly favoring linear alcohols with resultant augmented formation of aldehydes. Addition of increasing concentrations of synthetic Aβ(1–40) to ERAB/HADH II diminished NADH-dependent reduction of *S*-acetoacetyl-CoA (Fig. 5*A*). Inhibition fit to a one-site competitive model with $K_i \approx 1.6 \pm 0.5$ μM (34). Similarly, Aβ suppressed ERAB/HADH II-mediated, NAD^+-dependent oxidation of octanol ($K_i \approx 2.6 \pm 0.3$ μM; Fig. 5*B*) and 17β-estradiol ($K_i \approx 3.2 \pm 0.2$ μM; Fig. 5*C*). Comparable results were obtained when Aβ(1–42) was used in place of Aβ(1–40) (data not shown). Such levels of Aβ that attenuated ERAB/HADH II activity toward each of these substrates were considerably higher than those required to occupy Aβ binding sites on ERAB/HADH II; the K_d for Aβ binding to ERAB/HADH II was ≈40–70 nM (see Fig. 3*B*). This was an important consideration, because intracellular Aβ would more likely be present at nanomolar levels than in the micromolar range. Thus, there is probably a secondary effect of binding of additional molecules of Aβ (or perhaps aggregated/fibrillar Aβ) to ERAB/HADH II, but these effects are distinct from the lower amounts of Aβ that occupy ERAB/HADH II binding sites.

Change in Subcellular Distribution of ERAB/HADH II and Generation of Reactive Aldehydes in an Aβ-rich Environment—In a previous study, we observed that exogenous Aβ induced a change in the subcellular distribution of ERAB/HADH II in neuroblastoma cells (15). This suggested the possibility that ERAB/HADH II might find different substrates and/or activate enzyme systems following its transposition to new sites within the cell. Because of the association of oxidant stress with AD (9, 25–31), we considered the possibility that following translocation within the cell, ERAB/HADH II participated in events generating reactive aldehydes, MDA and/or HNE, both of which have been observed in the brain of AD patients (26–32).

First, subcellular distribution of ERAB/HADH II in neuroblastoma cells transfected to overexpress ERAB/HADH II alone or ERAB/HADH II + βAPP(V717G) was studied. Confocal microscopy of neuroblastoma cells transfected with pcDNA3/ERAB, either wtERAB or mutERAB(Y168G/K172G), displayed ERAB/HADH II principally in endoplasmic reticulum and mitochondria (Fig. 6, *A–F,* shows results with wtERAB). The distribution of ERAB/HADH II (Fig. 6, *C* and *F*) overlapped (Fig. 6, *A* and *D*), in part, with an endoplasmic reticulum marker, PDI (Fig. 6*B*) and a mitochondrial marker (Fig. 6*E*). Consistent with these results, subcellular fractionation of neuroblastoma cells transfected with pcDNA3/wtERAB showed ERAB/HADH II antigen to be principally in fractions enriched for mitochondrial and endoplasmic re-

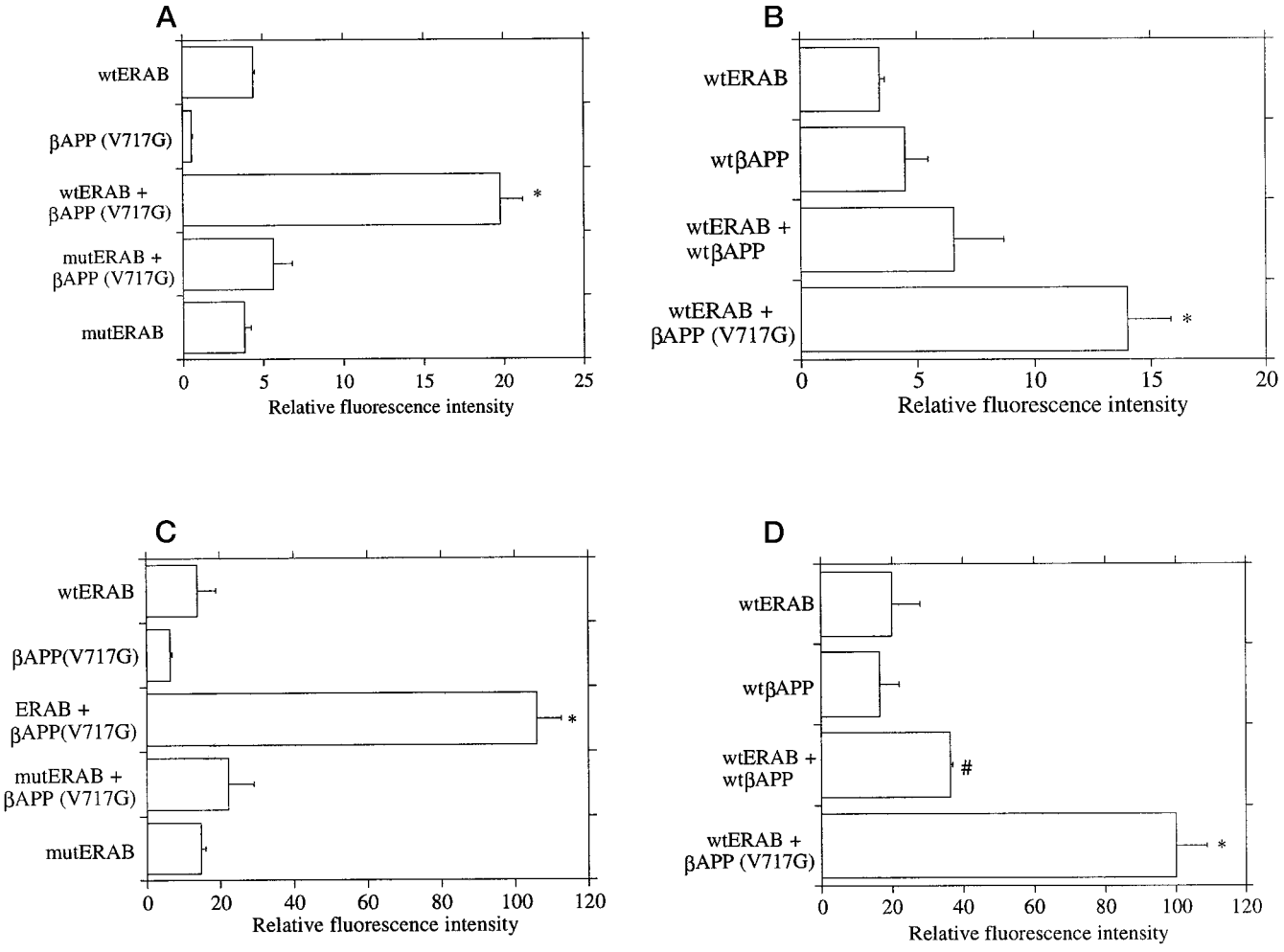

FIG. 9. **Quantitative analysis of MDA (*A* and *B*) and HNE (*C* and *D*) epitope expression in COS cells expressing wild-type or mutant ERAB/HADH II with or without βAPP(V717G) (*A* and *B*) or wild-type βAPP (wtβAPP) (*C* and *D*).** Data from experiments in Fig. 8 (for βAPP(V717G)) or from experiments in which primary data was not shown (for wtβAPP) were analyzed by the National Institutes of Health Image program. Relative fluorescence intensity (arbitrary units) is shown in COS cell cultures transfected with the indicated constructs. Each *bar* is labeled with the gene products overexpressed by transfection. * denotes $p < 0.01$; # denotes $p < 0.05$.

ticulum markers (Fig. 7*A*). The distribution of mutERAB in neuroblastoma cells similarly transfected with pcDNA3/mutERAB was comparable to that observed with wtERAB/HADH II, as seen in subcellular fractionation studies (Fig. 7*C*) and by confocal microscopy (data not shown). Cotransfection of neuroblastoma cells with pcDNA3/wtERAB and pAdlox/βAPP(V717G) displayed a different pattern of ERAB/HADH II antigen (Fig. 6, *G–L*). By confocal microscopy the altered distribution of ERAB/HADH II in cotransfectants (Fig. 6, *I* and *L*) was evident, with lesser amounts in endoplasmic reticulum (Fig. 6, *G* and *H*), although it was still in mitochondria (Fig. 6, *J* and *K*). Strikingly, in cotransfectants with pcDNA3/wtERAB and pAdlox/βAPP(V717G), ERAB/HADH II antigen seemed to be present in multiple sites within the cell, including the plasma membrane. In general, ERAB/HADH II antigen appeared to be more diffusely distributed in cotransfectants with some antigen in cell membrane, cytosol, and nuclear membrane and, in certain instances, associated with the nucleus. Subcellular fractionation studies showed a shift in ERAB/HADH II antigen to fractions rich in plasma membrane markers in cotransfectants (Fig. 7*B*). Similar results were obtained when mutERAB(Y168G/K172G) was overexpressed in place of wtERAB/HADH II (Fig. 7*D*). COS cells subjected to the cotransfection procedure and the same analysis as described above showed similar, though less striking results. Experiments in which wtβAPP was overexpressed along with wild-type ERAB/HADH II also showed translocation of ERAB/HADH II from endoplasmic reticulum-associated to plasma membrane-associated fractions (Fig. 7*E*), although to a somewhat lesser extent than was seen with mutant βAPP(V717G).

Having established that ERAB/HADH II changed its distribution in cells cotransfected to overexpress both ERAB/HADH II and βAPP(V717G), we next sought to determine whether reactive aldehydes (MDA or HNE) were formed under these conditions. COS cells overexpressing wtERAB/HADH II and βAPP(V717G) were studied for MDA and HNE epitopes using murine monoclonal antibodies and confocal microscopy. Cultures expressing either wtERAB/HADH II or βAPP(V717G) alone showed no increase in MDA (Fig. 8*A, I–III* and *IV–VI*, respectively) or HNE antigen (Fig. 8*B, I–III* and *IV–VI*, respectively). In contrast, cultures expressing both wtERAB/HADH II and βAPP(V717G) showed abundant MDA (Fig. 8*A, VII–IX*) and HNE antigen (Fig. 8*B, VII–IX*; quantitative analysis of this immunocytochemical data is shown in Fig. 9, *A* and *C*). In cotransfectants, the distribution of MDA and ERAB/HADH II (Fig. 8*A, VII*), or HNE and ERAB/HADH II (Fig. 8*B, VII*) antigen appeared to overlap, at least in part. ERAB/HADH II (Fig. 8, *A* and *B, IX*) and HNE or MDA (Fig. 8, *A* and *B, VIII*) were present in the cell membrane, as well as more diffusely throughout the cell. These experiments were also performed with mutERAB(Y168G/K172G) in place of wtERAB/HADH II (Fig. 8, *A* and *B, X–XV*). In contrast to the wild-type enzyme,

mutERAB (Fig. 8, *A* and *B, XII* and *XV*) did not generate elevated levels of either MDA or HNE epitopes (Fig. 8, *A* and *B, XI* and *XIV,* and Fig. 9). Thus, the integrity of the active site of ERAB/HADH II is required to support generation of reactive aldehydes, such as malondialdehyde and 4-hydroxynonenal, in cells cotransfected with βAPP(V717G). Further experiments were performed in which cultures were transfected to overexpress wtβAPP (in place of mutant βAPP) and wtERAB (Fig. 9, *B* and *D*). In these studies as well, there was an increase, although to a lesser extent, in generation of reactive aldehyde epitopes in cells expressing wtERAB + wtβAPP compared with cultures expressing either wtERAB or wtβAPP alone. For the latter studies, the increase in HNE epitopes (Fig. 9*D*) was more striking than that for MDA epitopes (Fig. 9*B*), although over many experiments, it was evident that both reactive aldehydes were produced at higher levels in cells cotransfected to overexpress wtERAB + wtβAPP than in cultures expressing either wtERAB or wtβAPP alone.

DISCUSSION

The properties of ERAB/L-3-hydroxyacyl-CoA dehydrogenase type II reveal an intriguing dichotomy for cellular homeostasis. On the one hand, enzyme activity as an L-3-hydroxyacyl-CoA dehydrogenase is consistent with ERAB/HADH II participation in metabolic homeostasis, namely in the fatty acid β-oxidation pathway. This concept is in accordance with previous reports demonstrating that bovine (17, 18) and, more recently, human (21) L-3-hydroxyacyl-CoA dehydrogenase reversibly catalyze the third reaction of the fatty acid β-oxidation cycle *in vitro*. Although inherited deficiencies of enzymes involved in fatty acid β-oxidation clearly have serious clinical consequences (19, 20), including a report of short chain 3-hydroxyacyl-CoA dehydrogenase deficiency (47), whether ERAB/HADH II has an important role in normal metabolic balance remains to be determined. ERAB/HADH II also has the capacity to dehydrogenate alcohol functions, including a range of linear alcohols, as well as 17β-estradiol. Although efficiency of the enzyme is less for the latter reactions than as an HADH, these data emphasize the potentially broad capacity of ERAB/HADH II to dehydrogenate a range of alcohol substrates. Whereas the physiologic significance of this property of ERAB/HADH II is not clear at this time, the potential of ERAB to metabolize 17β-estradiol, a neuro- and vascular-protective hormone (48–51), deserves further study. The reason for the apparent lack of ERAB/HADH type II activity as a 17β-hydroxysteroid dehydrogenase in the experiments of He *et al.* (21) may reflect differences in assay conditions and/or in the nature of the *E. coli*-derived protein.

From another vantage point, ERAB/HADH II takes on a quite different role in cells subjected to an environment rich in Aβ. Previously (15), we found that cell stress, following exposure of neuroblastoma cells to synthetic Aβ, was increased in cultures transfected to overexpress ERAB/HADH II. Cotransfection of the same ERAB/HADH II-expressing cells with a construct specifically generating cytosolic Aβ similarly enhanced cytotoxicity (15). Consistent with these data, blockade of ERAB/HADH II, following intracellular introduction of anti-ERAB $F(ab')_2$ using a liposome-based system, had a protective effect in the presence of Aβ (15). Because these previous experiments involved nonphysiologic exposure of cultured cells to Aβ and intracellular loading of foreign antibody fragments, we have extended our observations using a system in which cultured cells are simultaneously cotransfected with constructs encoding ERAB/HADH II and mutant βAPP(V717G). This system allows endogenous overexpression of both genes without other interventions; such cells suffer intense stress, evidenced by DNA fragmentation and generation of reactive aldehydes (MDA/HNE epitopes). Our results are unlikely to represent a general "endoplasmic reticulum stress response,"(52, 53) as similar cotransfection studies with ERAB/HADH II mutants devoid of enzymatic activity did not induce cell damage, although the level of expression of the transfected constructs was comparable.

Data from the cotransfection systems with pcDNA3/wtERAB and pAdlox/βAPP(V717G) suggest that ERAB/HADH II and, presumably, the product of cellular βAPP(V717G) metabolism, Aβ, interact with cytotoxic consequences for the host cell. The molecular mechanisms underlying such an interaction must be clarified in detail, because direct ERAB/HADH II binding to Aβ would suggest that Aβ generated in the lumen of the endoplasmic reticulum or other membrane-bound compartments could interact with ERAB/HADH II, the latter likely to be present on the cytosolic side of endoplasmic reticulum and in mitochondria. The apparently reduced potentiation of cytotoxicity when cultures were cotransfected with pcDNA3/wtERAB + pMT/wtβAPP, the latter in place of βAPP(V717G), suggests that high levels of cell-associated Aβ(1–42) generated with the mutant form of βAPP (36) accentuate toxicity in the presence of ERAB/HADH II. These data are also consistent with the possibility of an interaction, either direct or indirect, between ERAB/HADH II and Aβ. However, regardless of the precise mechanism by which ERAB/HADH II and Aβ interact, our data using this cotransfection system provide strong support for the concept that ERAB/HADH II enzymatic activity can exert deleterious effects in cells overexpressing βAPP. Thus, three ERAB/HADH II mutants that were devoid of enzymatic activity and expressed comparably to wtERAB/HADH II showed dramatically reduced DNA fragmentation in cotransfection experiments with pAdlox/βAPP(V717G), compared with native ERAB/HADH II. Because Aβ interaction with these enzymatically inactive ERAB/HADH II mutants was similar to that observed with wtERAB/HADH II, the enzymatic activity of ERAB must be differentiated from those determinants that mediate binding of Aβ. In accordance with this concept is our finding that ERAB/HADH II binding sites for Aβ are half-maximally occupied at a peptide concentration of ≈40–70 nM, whereas Aβ suppression of ERAB/HADH II enzymatic activity occurs at much higher concentrations, ≈2–3 μM. The latter levels of Aβ are unlikely to be present within cells, and, taken together, the data suggest that ERAB/HADH II binding to Aβ may modulate other properties of the molecule, such as its localization within the cell.

We hypothesize that when lower levels of Aβ are present in the brain, cytotoxicity may not be due solely to the amyloidogenic peptide itself, but may be amplified by cellular cofactors such as ERAB/HADH II. By directly forming a complex with ERAB/HADH II and/or indirectly (through undefined Aβ-mediated changes in cellular properties) modulating enzymatically active ERAB/HADH II function/localization, we increased cellular vulnerability. Taken together, the combination of Aβ binding properties and generalized alcohol dehydrogenase activity, in addition to HADH activity, lead us to propose the new name Aβ binding alcohol dehydrogenase or ABAD to better describe the unusual properties of the enzyme previously referred to as ERAB or HADH II.

Acknowledgment—We thank Dr. Gabriel Godman (Columbia University) for efforts and advice during the performance of these studies and preparation of the manuscript.

REFERENCES

1. Sisodia, S. S., and Price, D. L. (1995) *FASEB J.* **9,** 366–370
2. Selkoe, D. J. (1994) *Annu. Rev. Neurosci.* **17,** 489–517
3. Morrison, J., and Hof, P. (1997) *Science* **278,** 412–419
4. Selkoe, D. J. (1994) *J. Neuropathol. Exp. Neurol.* **53,** 438–447
5. Lendon, C., Ashall, F., and Goate, A. (1997) *J. Am. Med. Assoc.* **277,** 825–831

6. Hardy, J. (1997) *Trends Neurosci.* **20,** 154–159
7. Hensley, K., Carney, J., Mattson, M., Aksenova, M., Harris, M., Wu, J., Floyd, R., and Butterfield, D. (1994) *Proc. Natl. Acad. Sci. U. S. A.* **91,** 3270–3274
8. Mattson, M., and Goodman, Y. (1995) *Brain Res.* **676,** 219–224
9. Mark, R., Blanc, E., and Mattson, M. (1996) *Mol. Neurobiol.* **12,** 915–924
10. Yan, S.-D., Chen, X., Fu, J., Chen, M., Zhu, H., Roher, A. Slattery, T., Zhao, L., Nagashima, M., Morser, J., Migheli, A., Nawroth, P., Stern, D., and Schmidt, A.-M. (1996) *Nature* **382,** 685–691
11. Yan, S.-D., Zhu, H., Fu, J., Yan, S.-F., Roher, A., Tourtellotte, W., Rajavashisth, T., Chen, X., Stern, D., and Schmidt, A.-M. (1997) *Proc. Natl. Acad. Sci. U. S. A.* **94,** 5296–5301
12. Paresce, D., Ghosh, R., and Maxfield, F. (1996) *Neuron* **17,** 553–565
13. El-Khoury, J., Hickman, S., Thomas, C., Cao, L., Silverstein, S., and Loike, J. (1996) *Nature* **382,** 716–719
14. Yaar, M., Zhai, S., Pilch, P., Doyle, S., Eisenhauer, P., Fine, R., Gilchrest, B. (1997) *J. Clin. Invest.* **100,** 2333–2340
15. Yan, S.-D., Soto, C., Chen, X., Zhu, H., Al-Mohanna, F., Collison, K., Zhu, A., Stern, E., Saido, T., Tohyama, M., Ogawa, S., Roher, A., and Stern, D. (1997) *Nature* **389,** 689–695
16. Schembri, M., Bayly, R., and Davies, J. (1995) *J. Bacteriol.* **177,** 4501–4507
17. Furuta, S., Kobayashi, A., Miyazawa, S., and Hashimoto, T. (1997) *Biochim. Biophys. Acta* **1350,** 317–324
18. Kobayashi, A., Jiang, L., and Hashimoto, T. (1996) *J. Biochem.* **119,** 775–782
19. Roe, C., and Coates, P. (1995) in *The Metabolic Basis of Inherited Disease* (Scriver, C., Beaudet, L., Sly, W., and Vaye, D., eds) pp. 1501–1533, McGraw-Hill, Inc., New York
20. Eaton, S., Barlett, K., and Pourfarzam, M. (1996) *Biochem. J.* **320,** 345–357
21. He, X.-Y., Schulz, H., and Yang, S.-Y. (1998) *J. Biol. Chem.* **273,** 10741–10746
22. Rosenfeld, M., Palinski, W., Herttula, S., Butler, S., and Witztum, J. (1990) *Arteriosclerosis* **10,** 336–349
23. Palinski, W., Herttula, S., Rosenfeld, M., Butler, S., Socher, S., Parthasarathy, S., Curtiss, L., and Witztum, J. (1990) *Arteriosclerosis* **10,** 325–335
24. Palinski, W., Koschinsky, T., Butler, S., Miller, E., Vlassara, H., Cerami, A., and Witztum, J. (1995) *Atheroscler. Thromb. Vasc. Biol.* **15,** 571–582
25. Horie, K., Miyata, T., Maeda, K., Miyata, S., Sugiyama, S., Sakai, H., van Ypersele de Strihou, C., Monnier, V. M., Witztum, J. L., and Kurokawa, K. (1997) *J. Clin. Invest.* **100,** 2995–3004
26. Smith, M., Sayre, L., Monnier, V., and Perry, G. (1995) *Trends Neurosci.* **18,** 172–176
27. Smith, C., Carney, P., Starke-Reeds, P., Oliver, C., Stadtman, E., Floyd, R., and Markesbery, W. (1991) *Proc. Natl. Acad. Sci. U. S. A.* **88,** 10540–10543
28. Smith, M., Kutty, R., Rochey, P., Yan, S.-D., Stern, D., Chader, G., Wiggert, B., Petersen, R., and Perry, G. (1994) *Am. J. Pathol.* **145,** 42–47
29. Hensley, K., Hall, N., Subramaniam, R., Cole, P., Harris, M., Aksenov, M., Aksenova, M., Gabbita, S., Wu, J., Carney, J., Lovell, M., Markesbery, W., and Butterfield, D. (1995) *J. Neurochem.* **65,** 2146–2156
30. Yan, S.-D., Yan, S.-F., Chen, X., Fu, J., Chen, X., Kuppusamy, P., Yan, S.-H., Smith, G., Perry, G., Nawroth, P., Godman, Zweier, J., and Stern, D. (1995) *Nat. Med.* **1,** 693–699
31. Smith, M., Perry, G., Richey, P., Sayre, L., Anderson, V., Beal, M., and Kowall, N. (1996) *Nature* **382,** 120–121
32. Takedo, A., Yasuda, T., Miyata, T., Mizuno, K., Li, M., Yoneyama, S., Horie, K., Maeda, K., and Sobue, G. (1996) *Neurosci. Lett.* **221,** 17–20
33. Harlow, E., and Lane, D. (1988) *Antibodies: A Laboratory Manual*, Cold Spring Harbor Laboratory, New York
34. Segel, I. H. (1975) *Enzyme Kinetics, Behavior, and Analysis of Rapid Equilibrium and Steady-State Enzyme Systems*, Wiley-Interscience, New York
35. Klotz, I., and Hunston, D. (1984) *J. Biol. Chem.* **259,** 10060–10062
36. Wild-Bode, C., Yamazaki, T., Capell, A., Leimer, U., Steiner, H., Ihara, Y., and Haass, C. (1997) *J. Biol. Chem.* **272,** 16085–16088
37. Uyttendaele, H., Marazzi, G., Wu, G., Yan, Q., Sassoon, D., and Kitajewski, J. (1996) *Development* **122,** 2251–2259
38. Bonthron, D., Handin, R., Kaufman, R., Wasley, L., Orr, E., Mitsock, L., Ewenstein, B., Loscalzo, J., Ginsburg, D., and Orkin, S. (1986) *Nature* **324,** 270–273
39. Borchelt, D., Thinakaran, G., Eckman, C., Lee, M., Davenport, F., Ratovitsky, T., Prada, C.-M., Kim, G., Seekins, S., Yager, D., Slunt, H., Wang, R., Seeger, M., Levey, A., Gandy, S., Copeland, N., Jenkins, N., Price, D., Younkin, S., and Sisodia, S. (1996) *Neuron* **17,** 1005–1013
40. Kuwabara, K., Matsumoto, M., Ikeda, J., Hori, J., Ogawa, S., Maeda, Y., Kitagawa, K., Imuta, N., Kinoshita, T., Stern, D. M., Yanagi, H., and Kamada, T. (1996) *J. Biol. Chem.* **271,** 5025–5032
41. Du, Y., Dodel, R., Bales, K., Jemerson, R., Hamilton-Byrd, E., and Paul, S. (1997) *J. Neurochem.* **69,** 1382–1388
42. Cook, D., Forman, M., Sung, J., Leight, S., Iwatsubo, T., Lee, V., and Doms, R. (1997) *Nat. Med.* **3,** 1021–1023
43. Hartmann, T., Bieger, S., Bruhl, B., Tienari, P., Ida, N., Allsop, D., Roberts, G., Masters, C., Cotti, C., Unsicher, K., and Beyreuther, K. (1997) *Nat. Med.* **3,** 1016–1020
44. Tienari, P., Ida, N., Ikonen, E., Simons, M., Weidemann, A., Multhaup, G., Masters, C., Dotti, C., and Beyreuther, K. (1997) *Proc. Natl. Acad. Sci. U. S. A.* **94,** 4125–4130
45. Xu, H., Sweeney, D., Wang, R., Thinkaran, G., Lo, A., Sisodia, S., Greengard, P., and Gandy, S. (1997) *Proc. Natl. Acad. Sci. U. S. A.* **94,** 3748–3752
46. Shoji, M., Golde, T., Ghiso, J., Cheung, T., Estes, S., Shaffer, L., Cai, X.-D., McKay, D., Tintner, R., Frangione, B., and Younkin, S. (1992) *Science* **258,** 126–129
47. Tein, I., DeVivo, D. C., Hale, D. E., Clarke, J. T., Zinman, H., Laxer, R., Shore, A., and DiMauro, S. (1991) *Ann. Neurol.* **30,** 415–419
48. Tang, M.-X., Jacobs, D., Stern, Y., Marder, K., Schofield, P., Gurland, B., Andrews, H., and Mayeux, R. (1904) *Lancet* **348,** 429–432
49. Behl, C., Widman, M., Trapp, T., and Holsboer, F. (1995) *Biochem. Biophys. Res. Commun.* **216,** 473–482
50. Gilligan, D. M., Badar, D. M., Panza, J. A., Quyyumi, A. A., and Cannon, R. O. (1995) *Am. J. Cardiol.* **75,** 264–268
51. Grodstein, F., Stampfer, M. J., Manson, J., Colditz, G. A., Willett, W. C., Rosner, B., Speizer, F. E., and Hennekens, C. H. (1996) *New Engl. J. Med.* **335,** 453–461
52. Pahl, H., and Baeuerle, P. (1996) *FEBS Lett.* **392,** 129–136
53. Pahl, H., and Baeuerle, P. (1997) *Trends Biochem. Sci.* **22,** 63–67